Chemical Engineering Science 147 (2016) 137–149

Contents lists available at ScienceDirect

Chemical Engineering Science

journal homepage: www.elsevier.com/locate/ces

An effective computation strategy for assessing operational flexibility of high-dimensional systems with complicated feasible regions

Vincentius Surya Kurnia Adi [a], Rosalia Laxmidewi [b,1], Chuei-Tin Chang [a,*]

[a] Department of Chemical Engineering, National Cheng Kung University, Tainan 70101, Taiwan, ROC
[b] Independent Scholar, Tainan 70146, Taiwan, ROC

HIGHLIGHTS

- A new approach is proposed to accurately evaluate the volumetric flexibility index.
- The feasible region can be nonconvex, disjoint or non-simply connected in high-dimensional space.
- Random line search provides representative characterization of domain boundaries.
- No prior information of geometric properties is required in the proposed approach.
- Extensive case studies with 2–7 uncertain parameters are provided.

ARTICLE INFO

Article history:
Received 23 July 2015
Received in revised form
16 December 2015
Accepted 14 March 2016
Available online 26 March 2016

Keywords:
Nonconvex region
Non-simply connected region
Disconnected region
Random line search
Delaunay triangulation
Volumetric flexibility index

ABSTRACT

The *volumetric flexibility index* (FI_v) of a chemical system can be viewed geometrically as the ratio between the hypervolume of feasible region and that of a hypercube bounded by the expected upper and lower limits of uncertain process parameters. Although several methods have already been developed to compute FI_v, none of them are effective for solving the high-dimensional problems defined in nonconvex, non-simply connected or disconnected regions. While the available shortcut approaches are not accurate enough, successful tuning of the algorithmic parameters is mandatory for producing credible estimates with the more elaborate existing strategies.

The above practical issues in volume estimation are thoroughly addressed in the present research. The most critical step in the proposed procedure is to characterize the feasible region accurately. To this end, the domain boundaries in parameter space are first identified with the feasible proximity points obtained by following a random line search algorithm. The Delaunay triangulation technique is then implemented to generate simplexes on the basis of such near-boundary points. By checking the centroids of these simplexes, the infeasible ones may be identified and eliminated. Finally, the hypervolumes of all feasible simplexes are summed to determine the volumetric flexibility index.

Extensive case studies with 2–7 uncertain parameters have been carried out to show the superior capabilities of the proposed computation strategies.

1. Introduction

Sources of uncertainties in a chemical process design are often multifaceted. They can usually be associated with either "internal" process parameters, such as the reaction rates and physical properties, or "external" ones, such as the qualities and flow rates of feed streams to a reactor. To account for the worst-case scenarios, Grossmann and his coworkers first proposed a formal definition of the operational feasibility/flexibility and developed a quantitative performance measure accordingly to facilitate process analysis (Grossmann and Floudas, 1987; Swaney and Grossmann, 1985a, 1985b). More specifically, their flexibility index (denoted in this paper as FI_s) was computed numerically by solving a multi-level optimization problem. Many researchers later successfully integrated such a metric in their design procedure, e.g., see Lima et al. (2010), Riyanto and Chang (2010), and Adi and Chang (2011). Thorough literature surveys on the related studies have already been conducted by Ierapetritou (2001, 2009).

It should be noted first that, only when the feasible region is convex, FI_s can be safely considered as a proper flexibility measure. This prerequisite requirement is clearly impractical since a wide

* Corresponding author.
E-mail address: ctchang@mail.ncku.edu.tw (C.-T. Chang).
[1] This co-author helped coding.

http://dx.doi.org/10.1016/j.ces.2016.03.028
0009-2509/

variety of chemical engineering models are nonlinear and, thus, nonconvexity is a common feature that cannot be ignored. Geometrically speaking, the traditional flexibility index can be regarded as an aggregated indicator of the distances between the given nominal point and all faces of the biggest inscribable hypercube inside the feasible region. Hence a feasible region may be grossly misrepresented by this indicator if the chosen nominal point is very far off from the center and/or the biggest inscribable hypercube is much smaller than the feasible region due to concavities.

Lai and Hui (2008) suggested to use an alternative metric, i.e., the volumetric flexibility index (denoted as FI_v), to complement the conventional approach. Essentially, this volumetric index can be viewed in 3-D as the volumetric fraction of the feasible region inside a cube bounded by the expected upper and lower limits of uncertain process parameters. Since the total volume of feasible region is calculated without the need to specify a nominal point and/or to identify the biggest inscribable cube in the feasible region, the magnitude of FI_v can be more closely linked to process flexibility in cases when the feasible regions are nonconvex. However, in practical applications, the feasible regions of such processes may be quite complex and sometimes odd shaped. More specifically, these geometric objects can be nonconvex, non-simply connected and even disconnected (Croft et al., 1991; Krantz, 1999; Banerjee and Ierapetritou, 2005). Thus, the accuracy of volumetric flexibility evaluation depends heavily on how well the region boundaries can be characterized.

In fact, quite a few algorithms have already been developed for computing the hypervolumes of nonconvex feasible regions in the *n*-dimensional space, and their pros and cons are briefly summarized as follows:

The simplicial approximation approach proposed by Goyal and Ierapetritou (2003) is not only quite accurate but also capable of handling nonconvex regions, while its drawbacks can be mainly attributed to the needs for a priori knowledge of the region shape and, also, repetitive iteration steps to generate the optimal boundary points; The α-shape surface reconstruction method (Banerjee and Ierapetritou, 2005) was designed to handle nonconvex and disjoint regions. By implementing this algorithm according to properly sampled points, one can generate a reasonable polygonal representation of the feasible domain. However, the accurate estimate of its hypervolume is attainable only if a suitable α-shape factor can be identified efficiently. Tuning of such an algorithm parameter in realistic applications can be very tricky, especially when the feasible regions are topologically complex; Zilinskas et al. (2006) used sample points which are uniformly distributed over a unit cube to identify the feasible region of a distillation train, but the corresponding hypervolume could not be quantified easily; Bates et al. (2007) utilized search cones to identify the feasible region with uniform sampling points. This approach is especially impractical for odd-shaped regions since it is imperative to strike a proper balance between having enough points to characterize the region well and having too many points as this can make the model fitting process unstable; By using a fixed number of auxiliary vectors, the hypervolume of a feasible region may be quickly determined with accuracy comparable to those of the other methods (Lai and Hui, 2008). Unfortunately, in cases when the nonconvex constraints are present, a serious deterioration in estimation accuracy can occur due to the relatively small number of auxiliary vectors used in computation; On the other hand, the subspace feasibility test suggested by the same authors is in principle the most accurate numerical strategy for hypervolume estimation if the size of each subspace can be made small enough. However, since these subspaces are created by evenly partitioning the *entire* hypercube bounded between the upper and lower parameter limits, some of the tests do not seem to be necessary if the boundaries of the feasible region can also be taken into consideration. Therefore, as the dimension of parameter space increases, the huge number of required subspaces can render the computation inefficient and overwhelming.

Finally, notice that it is possible to characterize the feasible region even when the closed-form model of a given process is not available through the use of surrogate-based feasibility analysis. The so-called *high-dimensional model representation* (HDMR) has been adopted in Banerjee and Ierapetritou (2002), Banerjee and Ierapetritou (2003) and Banerjee et al. (2010) for input–output mapping of such processes, while the Kriging-based methodology was later proposed by Boukouvala and Ierapetritou (2012) for essentially the same purpose. Although these methods are based on samples, the developments of surrogate models for black-box problems and problems with known explicit models have both been reported (Rogers and Ierapetritou, 2015a, 2015b). This approach involves developing a surrogate model to represent the feasibility function and using it to reproduce the feasible region. Note that the dependency on the sample accuracy and the proper surrogate model are crucial in this approach. Although the surrogate model is often less computationally expensive, it may lack the physical insights needed to accurately identify the potential debottlenecking measures. Notice that this is always an important incentive for locating the active constraint(s) in traditional flexibility analysis (Grossmann and Floudas, 1987). Moreover, while the surrogate models have been applied successfully for feasibility analysis, the resulting index values may not be identical to those of the traditional flexibility index (FI_S) or the volumetric flexibility index (FI_v) (Rogers and Ierapetritou, 2015a, 2015b). Hence, it is sometimes difficult to compare these different indices on the same basis.

All aforementioned implementation issues have been addressed in our studies. The proposed computation procedure is more effective for handling high-dimensional problems defined in complex (such as the non-simply connected or disconnected) regions. As mentioned before, the most critical step is concerned with accurate characterization of the feasible region. To this end, the domain boundaries in parameter space are depicted in this work with the feasible proximity points obtained according to a random line search algorithm. There are two main incentives for this practice. Firstly, as opposed to the *a priori* geometric knowledge required in Goyal and Ierapetritou (2003), this random search (Vempala, 2005) should be effective in sketching the operable region of a given process without the need for analyzing the nonconvex constraints in advance. Secondly, since two or more proximity points can be produced with a single line, the proposed strategy should outperform the other random search methods that generate and test one point at a time.

Note that it is important to obtain sample points near or at boundaries since the interior points are not needed in partitioning a high-dimensional feasible region and computing its hypervolume. For the former purpose, a Delaunay triangulation technique is applied to create simplexes according to the aforementioned proximity points. The centroid of every simplex is then checked for infeasibility, and the hypervolumes of all feasible ones can be summed for computing the volumetric flexibility index. This computation strategy can be carried out without repetitively tuning any algorithmic parameter and, also, the resulting estimates are expected to be at least as accurate as those obtained with any existing method. It should also be pointed out that the proposed solution strategy should be more efficient in the preliminary preparation stage since there are virtually no needs for constructing/modifying model formulations.

The remaining part of this article is organized as follows. Firstly, since the feasibility check is an essential calculation in evaluating the hypervolume, the model formulation of the corresponding optimization problem is given in Section 2 to facilitate clear illustration of the subsequent materials. Section 3 presents an integrated computation procedure, which includes the algorithms for producing feasible proximity points by the random line search, for generating the simplexes in a Delaunay triangulation scheme,

for calculating the hypervolume of a given feasible region and also the corresponding volumetric flexibility index. A number of case studies are then provided in the next section to demonstrate the feasibility and effectiveness of the proposed approach in producing accurate flexibility measures for high-dimensional systems with complex feasible regions. Extensive new results, which cannot be obtained with the available approaches, are also reported. Finally, the conclusions are drawn at the end of paper.

2. Feasibility check

As mentioned before, the feasibility check is an essential computation which is required at various stages of the flexibility evaluation process. In order to provide accurate explanation, the following label sets should be first defined:

$$\mathrm{I} = \{i | i \text{ is the label of an equality constraint}\} \tag{1}$$

$$\mathrm{J} = \{j | j \text{ is the label of an inequality constraint}\} \tag{2}$$

The general design model can be expressed accordingly as

$$h_i(\mathbf{d}, \mathbf{z}, \mathbf{x}, \boldsymbol{\theta}) = 0, \quad \forall\, i \in \mathbf{I} \tag{3}$$

$$f_j(\mathbf{d}, \mathbf{z}, \mathbf{x}, \boldsymbol{\theta}) \le 0, \quad \forall\, j \in \mathbf{J} \tag{4}$$

where, h_i is the ith equality constraint in the design model (e.g., the mass or energy balance equation for a processing unit); f_j is the jth inequality constraint in the design model (e.g., a capacity limit); $\mathbf{d}$ represents a vector in which all design variables are stored; $\mathbf{z}$ denotes the vector of *adjustable* control variables; $\mathbf{x}$ is the vector of state variables; $\boldsymbol{\theta}$ denotes the vector of uncertain parameters which are assumed to be bounded within a hypercube in the parameter space, i.e.

$$\boldsymbol{\theta}^L \le \boldsymbol{\theta} \le \boldsymbol{\theta}^U \tag{5}$$

Note that $\boldsymbol{\theta}^U$ and $\boldsymbol{\theta}^L$ respectively represent the vectors of expected upper and lower bounds of the uncertain parameters. It should also be noted that, although the uncertain parameters may be functions of some of the aforementioned design, control and/or state variables, these possibilities are excluded for simplicity in the present study.

It should be noted that, given a fixed design ($\bar{\mathbf{d}}$) and a particular point (say $\mathbf{b}$) in the parameter hypercube defined by Eq. (5), the feasibility of this given point cannot be confirmed in a straightforward fashion due to the presence of control variables (z) in the model constraints, i.e., (Eqs. (3) and 4). A mathematical programming model must be solved for this purpose. Specifically, this optimization problem can be expressed as

$$-\mathrm{P}\left(\bar{\mathbf{d}}, \mathbf{b}\right) = \min_{\mathbf{x},\mathbf{z}} \max_{j\in\mathrm{J}} f_j$$
$$s.\ t.$$
$$h_i\left(\bar{\mathbf{d}}, \mathbf{x}, \mathbf{z}, \mathbf{b}\right) = 0, \quad i \in \mathrm{I}. \tag{6}$$

If $\mathrm{P} \ge 0$, then the given point in parameter space can be considered as feasible and the corresponding control values will be denoted as $\bar{\mathbf{z}}$ throughout this paper. Notice that the aforementioned vector $\mathbf{b}$ can be either selected randomly or assigned deterministically and, also, the upper-level minimization calculation is introduced primarily to avoid producing erroneous negative P values that are associated with some of the feasible points near boundaries of the feasible region.

3. Integrated computation procedure

By integrating several software tools, computation of the volumetric flexibility index requires sequential implementation of five distinct steps: (1) placement of feasible proximity points with random line search, (2) generation of simplexes using the Delaunay triangulation strategy, (3) removal of infeasible simplexes, (4) calculation of total hypervolume, and (5) evaluation of volumetric flexibility index ($\mathrm{FI_v}$). A brief explanation of each step and also an overall flowchart are provided in the sequel:

3.1. Random line search

Clearly a precise geometric characterization of the nonconvex feasible region is the prerequisite of accurate $\mathrm{FI_v}$ evaluation. Several alternative strategies have already been developed for this purpose based on the ideas of simplicial approximation (Goyal and Ierapetritou, 2003), α-shape surface reconstruction (Banerjee and Ierapetritou, 2005), auxiliary vector and subspace feasibility test (Lai and Hui, 2008). Since, as mentioned before, these available methods may not be satisfactory in certain applications, a random line search algorithm has been developed in this work to place feasible points at or near the boundaries of the feasible region in the parameter space. Specifically, this search is realized by solving a mathematical programming model described in the sequel.

Let us first assume that a feasibility check has already been performed for a given design $\bar{\mathbf{d}}$ on a randomly generated vector $\mathbf{b}$ to obtain $\bar{\mathbf{z}}$. A second mathematical program can then be formulated accordingly after producing another random vector $\mathbf{a}$, i.e.

$$\mathrm{Q}\left(\bar{\mathbf{d}}, \bar{\mathbf{z}}, \mathbf{a}, \mathbf{b}\right) = \min_{\mathbf{x},t,j\in\mathrm{J}} s_j$$
$$s.\ t.$$
$$h_i\left(\bar{\mathbf{d}}, \mathbf{x}, \bar{\mathbf{z}}, \boldsymbol{\theta}\right) = 0, \quad i \in \mathrm{I};$$
$$f_j\left(\bar{\mathbf{d}}, \mathbf{x}, \bar{\mathbf{z}}, \boldsymbol{\theta}\right) + s_j = 0, \quad s_j \ge 0, \quad j \in \mathrm{J}$$
$$\boldsymbol{\theta} = \mathbf{a}t + \mathbf{b}, \quad +\infty > t > -\infty. \tag{7}$$

where s_j is the slack variable of inequality $j \in \mathrm{J}$ and t is the parametric variable for a straight line. If the optimal objective value is smaller than a designated threshold value ε, i.e., $\mathrm{Q} < \varepsilon$, then the corresponding vector(s) in the parameter space should be regarded as feasible proximity point(s) of the boundaries.

For illustration convenience, let us denote the total number of feasible proximity points targeted in a search and the maximum number of lines allowed per feasible point as N_{point} and N_{line} respectively. Although it is permissible to generate more than one line by pivoting at the same feasible point $\mathbf{b}$, it is preferrable to set N_{line} so as to maintain the maximum degree of randomness in the search. Note also that, since $\mathbf{b}$ must be feasible, at least one point on the line $\boldsymbol{\theta} = \mathbf{a}t + \mathbf{b}$ should be feasible, i.e., when $t = 0$. As a result, the vector $\mathbf{a}$ can be selected arbitrarily.

The corresponding search procedure can be outlined as follows:

1. Let $n = 0$ and $\Theta = \varnothing$.
2. Generate a random vector $\mathbf{b}$ within the parameter hypercube according to Eq. (5). Perform feasibility check on $\mathbf{b}$ by solving (Eqs. (3), (5), and 6).
3. If $\mathrm{P} < 0$, then go to step 2. Otherwise, save $\mathbf{b}$ and $\bar{\mathbf{z}}$, and then go the next step.
4. Let $k = 0$ and $\Omega = \varnothing$.
5. Generate an additional random vector $\mathbf{a}$ and solve Eq. (7).
6. If $\mathrm{Q} \ge \varepsilon$, then go to step 5. Otherwise, incorporate all solutions (i.e., the feasible proximity points) into the set Ω and go to the

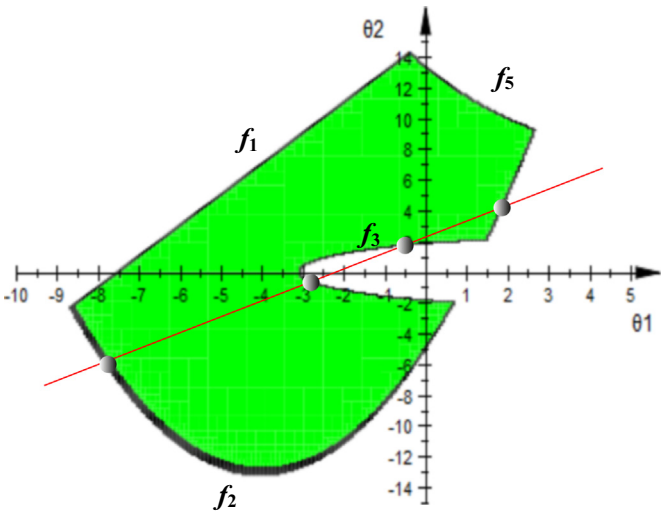

Fig. 1. Feasible region of motivating example.

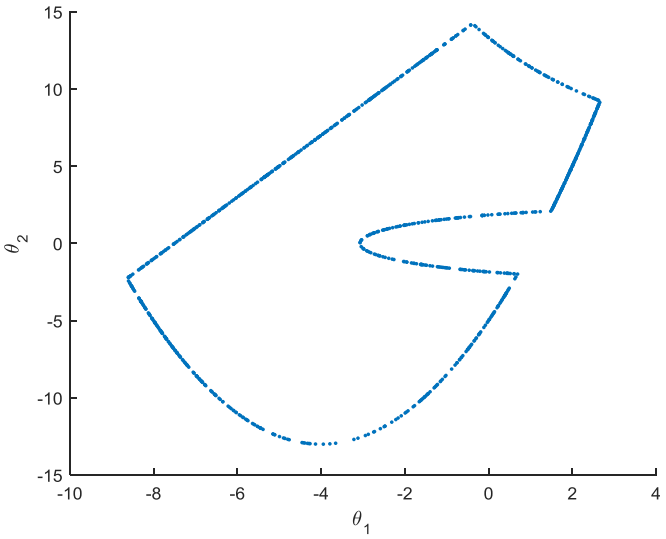

Fig. 2. Feasible proximity points generated in the motivating example.

next step.

7. Let $k = k + 1$. If $k \le N_{\text{line}}$, go to step 5. Otherwise, go to the next step.
8. Let $\Theta = \Theta \cup \Omega$ and $n = n + \text{card}(\Omega)$, where $\text{card}(\Omega)$ denotes the cardinality of set Ω. If $n \le N_{\text{point}}$, go to step 2. Otherwise, stop.

An obvious advantage of this search strategy is that at least two proximity points can be generated with a single line. For a conceptual understanding, let us consider a motivating example with the following five inequality constraints:

$$f_1 = \theta_2 - 2\theta_1 - 15 \le 0$$
$$f_2 = \frac{\theta_1^2}{2} + 4\theta_1 - 5 - \theta_2 \le 0$$
$$f_3 = 10 - \frac{(\theta_1 - 4)^2}{5} - \frac{\theta_2}{0.5} \le 0$$
$$f_4 = \theta_2 - 15 \le 0$$
$$f_5 = \theta_2(6 + \theta_1) - 80 \le 0 \qquad (8)$$

Fig. 1 shows the corresponding feasible region and note that there are two nonconvex constraints, i.e., f_3 and f_5. In the original problem statement (Goyal and Ierapetritou, 2003), a nominal point

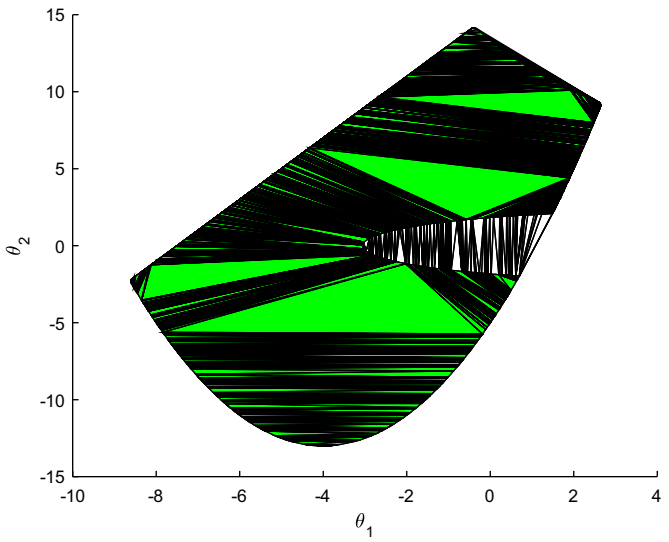

Fig. 3. Delaunay triangulation scheme obtained from the proximity points in Fig. 2.

of $(\theta_1^N, \theta_2^N) = (-2.5, 0)$ was adopted with expected deviations of $(\Delta\theta_1^+, \Delta\theta_1^-) = (7.5, 7.5)$ and $(\Delta\theta_2^+, \Delta\theta_2^-) = (15, 15)$. In this figure, a single random line is drawn to show the possibility of getting multiple solutions with the same **a** and **b**. The proposed search algorithm was coded and implemented on MATLAB-GAMS platform (Dirkse et al., 2014; Matlab, 2014; Rosenthal, 2014) to produce 1000 feasible proximity points with $N_{\text{point}} = 1000$ and $N_{\text{line}} = 1$ (see Fig. 2). It can be observed that the boundaries of the feasible region are well characterized and thus an accurate estimate of its boundary may be obtained accordingly.

3.2. Delaunay triangulation

The Delaunay triangulation strategy has been widely adopted for scientific computing in diverse applications. Published examples include particle collision detection (Yazdchi et al., 2009), computer vision (Dinas and Banon, 2014), protein interaction (Zhou and Yan, 2012) and particle tracking (Chen et al., 2014), etc. While there are many other computer algorithms available, it is its favorable geometric properties that make this particular one useful in the present work. The constrained Delaunay triangulation strategy can in fact be implemented in high dimensions without any difficulties, as the algorithm is quite mature and has already been embedded in commercial software (Barber et al., 1996; Delaunay triangulation, 2014). The 2-dimensional dataset presented previously in Fig. 2 are again used here as an example for illustration. The simplexes (triangles) shown in Fig. 3 were obtained by direct implementation of the Delaunay procedure using the MATLAB built-in function "delaunayn" (delaunayn, 2014). Note that some of the simplexes are actually located outside the feasible region.

3.3. Infeasible simplexes

For illustration convenience, let us assume that coordinate data of the aforementioned proximity points in n-dimensional space can be stored in a N_{prox}–by–n matrix **X**, and each row vector of **X** represents one such point. The MATLAB function "delaunayn" basically generates a list of N_{simp} simplexes in such a way that no data points in **X** are located inside the circumsphere of any simplex (delaunayn, 2014). This Delaunay triangulation list T is essentially a N_{simp}–by–$n + 1$ array in which each row contains the row indices of **X** for the $n + 1$ vertices of a simplex., i.e., simplex k

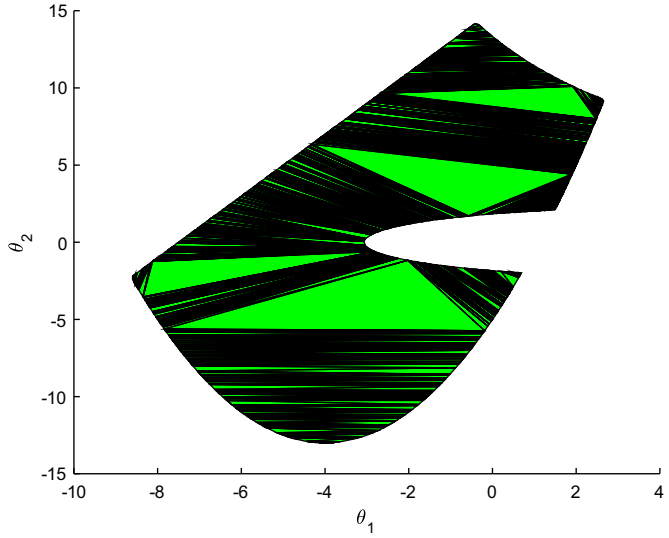

Fig. 4. Enhanced triangulation scheme obtained from Fig. 3.

in the triangulation scheme is uniquely associated with the kth row of list T and its ith element $T_i^k (i = 0, 1, \cdots, n)$ is with row vector T_i^k in $\mathbf{X}$.

Consequently, the centroid $\bar{\boldsymbol{\theta}}^k$ of simplex k can be calculated using the simple formula (Johnson, 2007) given below:

$$\bar{\boldsymbol{\theta}}^k = \frac{1}{n+1} \sum_{i=0}^{n} \mathbf{x}_i^k \tag{9}$$

where, $\mathbf{x}_i^k$ denotes row vector T_i^k in $\mathbf{X}$, i.e., the coordinate vector for vertex i of simplex k. Given a fixed design ($\bar{\mathbf{d}}$) and a centroid $\bar{\boldsymbol{\theta}}^k$, the mathematical programming model given in Eq. (6) can be solved to determine the feasibility of the simplex k with the corresponding centroid $\bar{\boldsymbol{\theta}}^k$. A simplex can be retained only when the corresponding $P \geq 0$. Fig. 4 shows the enhanced triangulation scheme obtained by removing the infeasible simplexes in Fig. 3. Note that three types of numerical errors may arise from the aforementioned triangulation and elimination procedures. The first is originated from feasible regions not covered by the simplexes, while the other two are associated with simplexes that can be divided into multiple parts by one or more boundary. In the latter two cases, a partially infeasible simplex may be either kept or rejected depending on the test result of its centroid. To achieve an acceptable level of accuracy in estimating the total hypervolume of feasible region, a sufficient number of proximity points should therefore be utilized and this number can be properly determined with the heuristic rule developed later in Subsection 4.3.

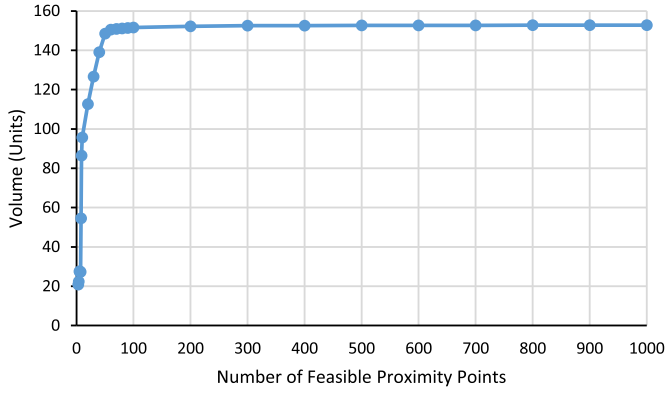

Fig. 5. Effects of increasing proximity points in motivating example.

3.4. Hypervolume calculation

The hypervolume of simplex $k (k = 1, 2, \cdots, N_{\text{simp}})$ can be computed in a straightforward fashion with the following formula (Stein, 1966; Burkardt, 2014):

$$V^k = \frac{1}{n!} \left| \det \left[\left(\mathbf{x}_1^k - \mathbf{x}_0^k\right)^T \left(\mathbf{x}_2^k - \mathbf{x}_0^k\right)^T \cdots \left(\mathbf{x}_n^k - \mathbf{x}_0^k\right)^T \right] \right| \tag{10}$$

where, each column of the n-by-n matrix is the transpose of difference between two row vectors representing vertex i ($i = 1, 2, \cdots, n$) and the reference vertex $\mathbf{x}_0^k$ respectively. The total hypervolume of the feasible region V_{fr} can therefore be calculated easily by summing those of all feasible simplexes. For the motivating example, analytical integration can be performed and the theoretical area of the feasible region can be determined to be 152.76 units. On the other hand, the total area of all triangles in Fig. 3 can be found to be 165.93 units by making use of Eq. (10), while that of the feasible region in Fig. 4 is 152.7442 units (which is 99.99% of the theoretical value).

For the motivating example, the estimated "volume" is plotted against the number of feasible proximity points (from 3 to 1000) in Fig. 5. It can be observed that the proposed method underestimates the feasible volume initially until reaching $N_{\text{point}} \approx 100$ and, thus, 10^2 appears to be a proper lower bound for the number of feasible proximity points.

3.5. Flexibility measure

According to Lai and Hui (2008), the volumetric flexibility index FI_v should be calculated according to the formula below:

$$\text{FI}_\text{v} = \frac{V_{\text{fr}}}{V_{\text{ur}}} \tag{11}$$

where, V_{ur} is the hypercube volume bounded by the expected upper and lower limits of uncertain process parameters. Thus, the exact value of volumetric flexibility index for the motivating example is

$$\text{FI}_\text{v} = \frac{152.76}{(7.5 + 7.5) \times (15 + 15)} = 0.34 \tag{12}$$

Since this problem has already been solved in several previous studies, it is therefore necessary to first present a summary of all available results. The approximated area of feasible region was found by Goyal and Ierapetritou (2003) with the simplicial approximation approach to be 129.69 units (which is only 84.90% of the theoretical value) and therefore the corresponding estimate of FI_v is 0.29. Using the α-shape surface reconstruction algorithm, Banerjee and Ierapetritou (2005) only reported the sampled feasible points without the resulting area. For comparison purpose, the α-shape surface reconstruction computation has been repeated in this study with the built-in MATLAB function "alphaShape" (alphaShape, 2014) on the basis of 3356 evenly distributed points and a critical alpha radius of 0.1694 (criticalAlpha, 2014). The estimated area in this case is 148.58 units (which is 97.26% of the theoretical value) and, thus, the corresponding FI_v is 0.33. Lai and Hui (2008) also studied the same problem by using the auxiliary vector approach with two alternative objectives, i.e., (1) maximizing the sum of lengths of the position vectors that represent the interception points and (2) maximizing the sum of squares of the distances between interception points and a reference point. The former yielded an area estimate of 148.03 units (96.90% of the theoretical value) and the corresponding FI_v is 0.33, while the latter produced an overestimated area of 155.75 units (101.96% of the theoretical value) and an

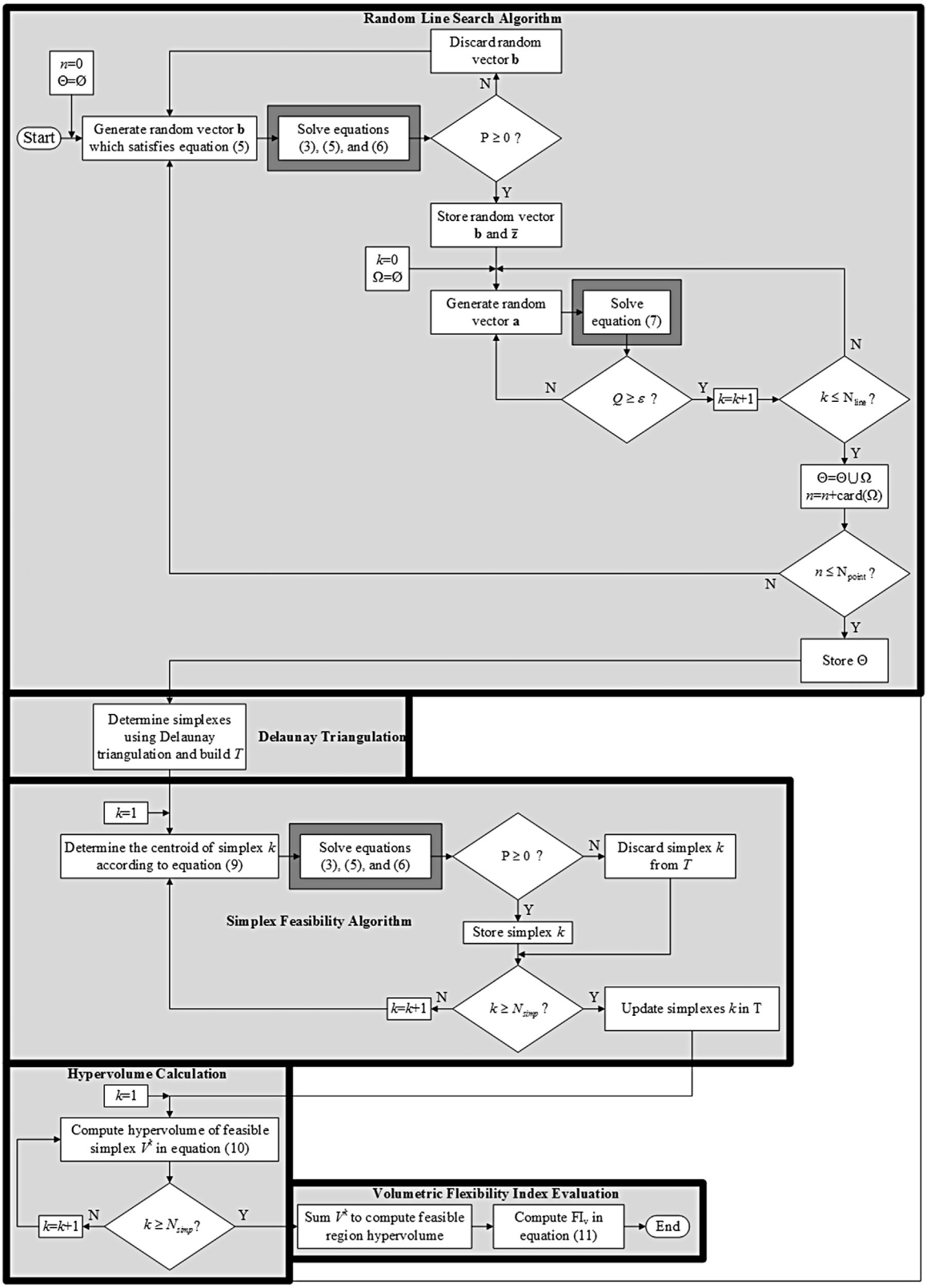

Fig. 6. Flowchart of overall procedure.

optimistic flexibility index of 0.35. As mentioned before, the total area of feasible simplexes in Fig. 4 was found to be 152.7442 (99.99% of the theoretical value) and, thus, the resulting flexibility measure FI_v (0.34) should be more accurate than any of the aforementioned methods.

3.6. Integrated computation procedure

The aforementioned algorithms can be integrated into a single procedure for evaluating the volumetric flexibility index, and this procedure is concisely described with the flowchart given in Fig. 6.

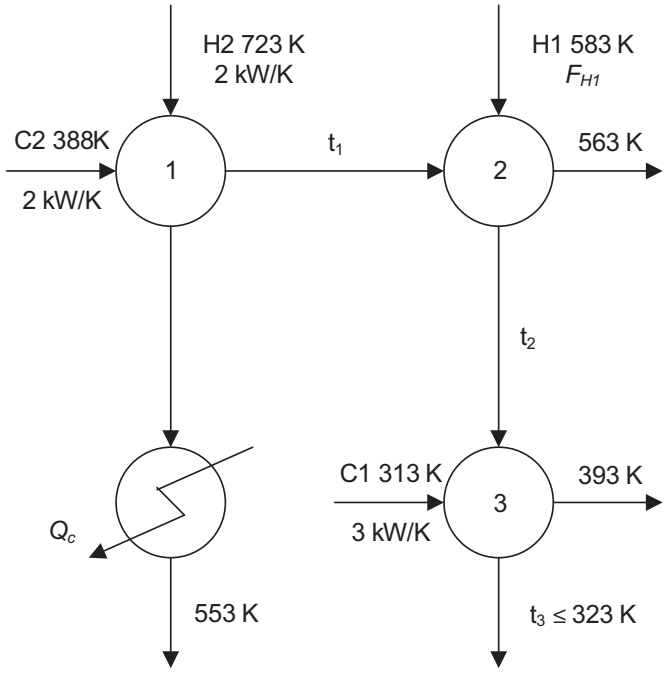

Fig. 7. Heat exchanger network studied in Grossmann and Floudas (1987).

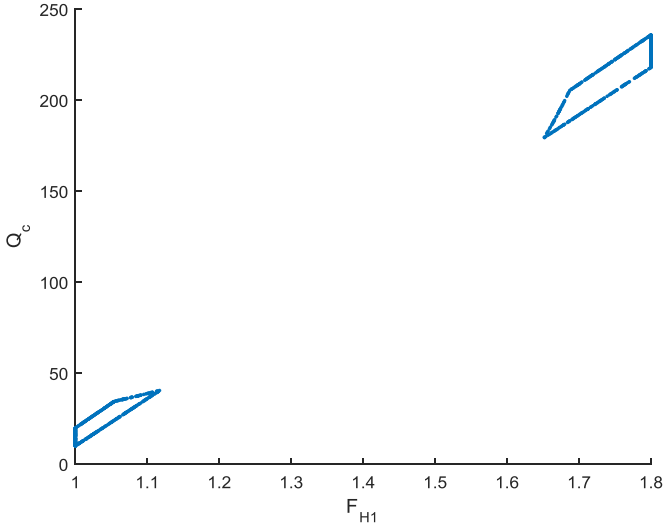

Fig. 8. Feasible proximity points generated for expanded feasible region.

The optimization runs performed by GAMS are marked with blocks enclosed by thick dark-grey lines in this figure, while the computations carried out with MATLAB codes are placed in blocks against light-grey background. Although this flowchart is self-explanatory, its steps are still briefly described as follows for the sake of illustration completeness:

(1) The first step is the random line search. On the MATLAB-GAMS platform, the corresponding computations produce the data set Θ that contains all required feasible proximity points; (2) The feasible proximity points in Θ are then triangulated using MATLAB N-D Delaunay triangulation built-in function "delaunayn" in MATLAB to generate the triangulation list T; (3) The centroid of every simplex in T is checked for feasibility and the infeasible ones are deleted. The triangulation list T is then updated accordingly; (4) The hypervolumes of all simplexes in the updated list T are computed and summed to estimate the hypervolume of feasible region; (5) The corresponding the volumetric flexibility index is finally evaluated according to its definition.

4. Case studies

The examples in this section were selected to demonstrate the effectiveness of the proposed computation strategies in handling disjoint, non-simply connected and high-dimensional feasible regions. The aforementioned computation procedure was implemented on a computer system with the following specifications: Acer Veriton P530 F2, 2x Intel® Xeon® CPU E5-2620 v2@2.10 GHz (12 cores), 64 GB RAM, Windows 10 64 bit, MATLAB 2015b, and GAMS 24.5.3 (August 2015). The default values of ε and N_{line} for the line search were chosen to be 10^{-6} and 1 respectively. In all cases reported below, the time needed for each MATLAB-GAMS call was less than 0.001 second. For the 7D problem in subsection 4.6, the elapsed time for triangulation was less than 2 h and the entire computation process lasted less than 5 h.

4.1. Disjoint feasible region

To demonstrate the capability of the proposed approach in evaluating disconnected feasible regions, let us consider the heat exchanger network (HEN) in Fig. 7 (Grossmann and Floudas, 1987). The original model formulation was obtained by eliminating the state variables with the equality constraints, i.e.

$$\begin{aligned} f_1 &= -25F_{H1} + Q_c - 0.5Q_cF_{H1} + 10 \leq 0 \\ f_2 &= -190F_{H1} + Q_c + 10 \leq 0 \\ f_3 &= -270F_{H1} + Q_c + 250 \leq 0 \\ f_4 &= -260F_{H1} - Q_c - 250 \leq 0 \end{aligned} \tag{13}$$

Q_c in these constraints is the cooling load which has been treated as a positive-valued control variable, while F_{H1} is the heat capacity flow rate of hot stream H1 and it is regarded as the only uncertain parameter in this problem. It is also assumed that the uncertain parameter has a nominal value of $F_{H1}^N = 1.4$ kW/K and the expected positive and negative deviations (i.e., ΔF_{H1}^+ and ΔF_{H1}^-) are both set at 0.4 kW/K. In the space formed by both the control variable and uncertain parameter, the *expanded* feasible region defined by Eq. (13) actually consists of two disconnected domains (Grossmann and Floudas, 1987). Note that its exact total area, i.e., 3.15 units, can be determined by analytical integration. Note also that the simplicial approximation approach requires a priori identification of the nonconvex constraint(s), i.e., f_1, that causes the division of the feasible region. The total area of disjoint feasible regions was estimated by Goyal and Ierapetritou (2003) to be 1.84 units, which is 58.41% of the actual value. Since in this work their flexibility measure was defined differently, their index value is not presented here for comparison. On the other hand, the proposed search algorithm has also been implemented to characterize the expanded feasible region mentioned above. A total of 1000 feasible proximity points were generated by treating Q_c as a pseudo-parameter to mimic the feasible boundaries (see Fig. 8). The simplexes shown in Fig. 9 were obtained by Delaunay triangulation strategy and the corresponding total area is 3.14 units (99.68% of the actual value).

Finally, it should be noted that the present problem is actually 1-D since there is only 1 uncertain parameter F_{H1}. The actual feasible region is just two separated line segments which can be generated by projecting the expanded region onto F_{H1} axis. Specifically, from the intersection points of f_1 and f_4, one can easily locate the upper limit of the segment on the left and the lower limit on the right and their values are 1.118 and 1.651 respectively. Therefore, the exact value of 1-D FI_v is

$$\text{FI}_\text{v} = \frac{(1.118 - 1) + (1.8 - 1.651)}{0.8} = 0.334 \tag{14}$$

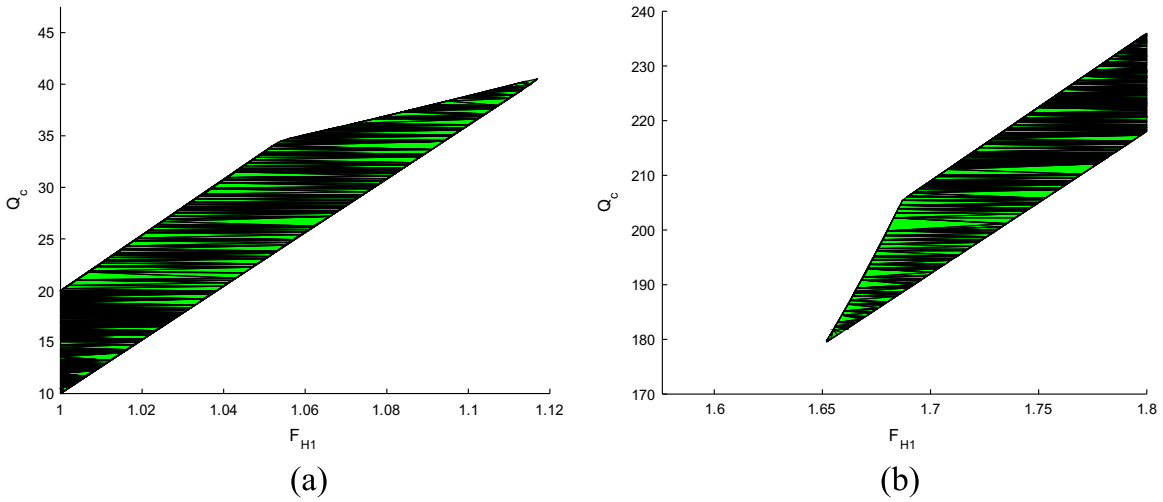

Fig. 9. Delaunay triangulation schemes obtained from Fig. 8: (a) Left; (b) Right.

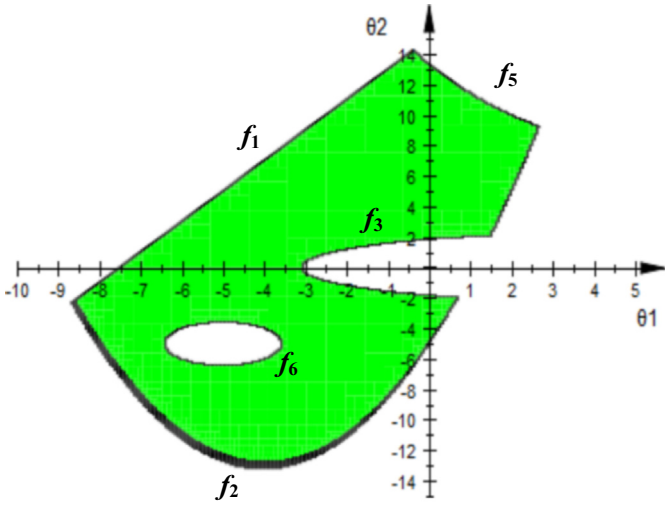

Fig. 10. Feasible region of 2D non-simply connected example.

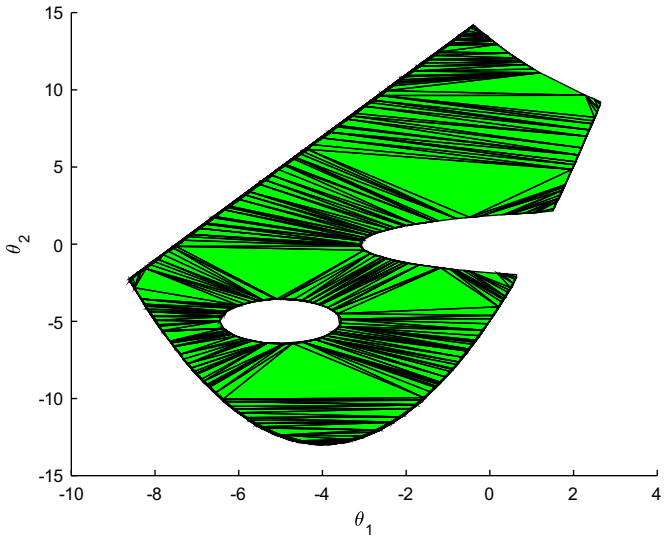

Fig. 12. Delaunay triangulation scheme obtained from Fig. 11.

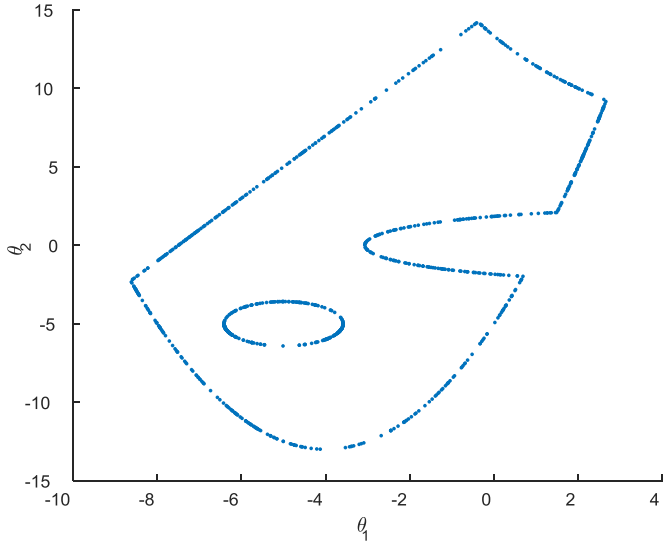

Fig. 11. 10^3 feasible proximity points generated in 2D non-simply connected example.

Based on the data points generated from random hit and run search (see Fig. 9), the first part spans the interval [1, 1.117] and the second [1.652, 1.8]. Thus the corresponding value of FI_v is

$$FI_v = \frac{(1.117 - 1) + (1.8 - 1.652)}{0.8} = 0.331 \tag{15}$$

which corresponds to 99.10% of the actual FI_v. This result shows that the random line search algorithm produce a reliable high accuracy prediction of the feasible region.

4.2. 2D non-simply connected feasible region

To show the effectiveness of the proposed approach in handling the non-simply connected regions, let us revisit the motivating example and introduce an additional constraint:

$$f_6 = -(\theta_1 + 5)^2 - (\theta_2 + 5)^2 + 2 \le 0 \tag{16}$$

Fig. 10 shows the corresponding feasible region. By performing analytical integration, the exact area of this region can be determined to be 146.48 units. Thus, the true value of volumetric flexibility index should be

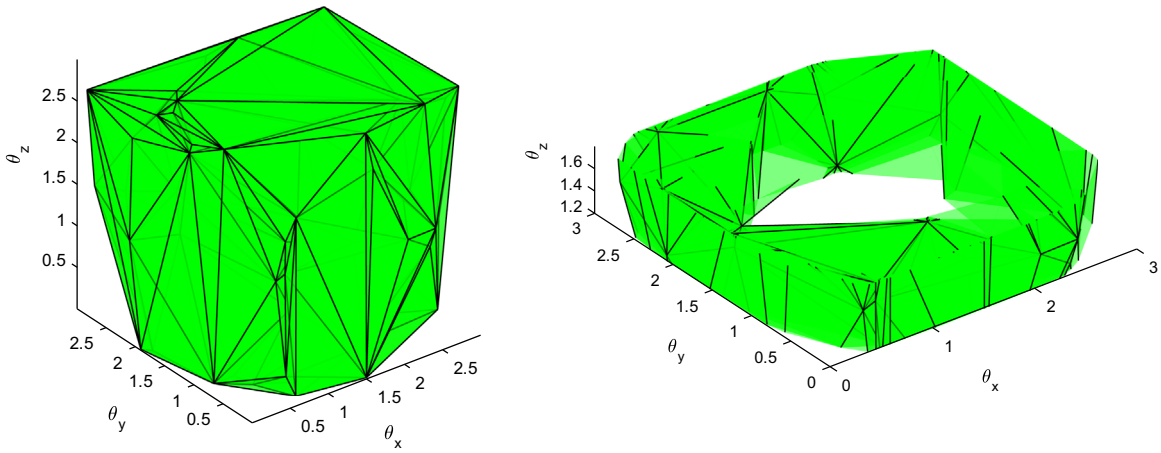

Fig. 13. Left – Triangulation scheme constructed according to 10^2 randomly generated proximity points; Right – Partial triangulation scheme shown for a limited range of θ_z.

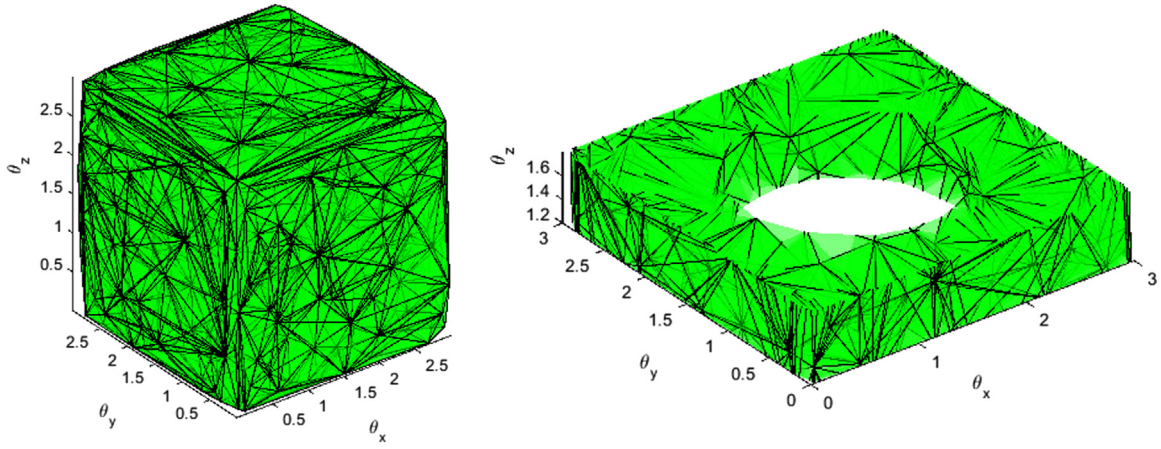

Fig. 14. Left – Triangulation scheme constructed according to 10^3 randomly generated proximity points; Right – Partial triangulation scheme shown for a limited range of θ_z.

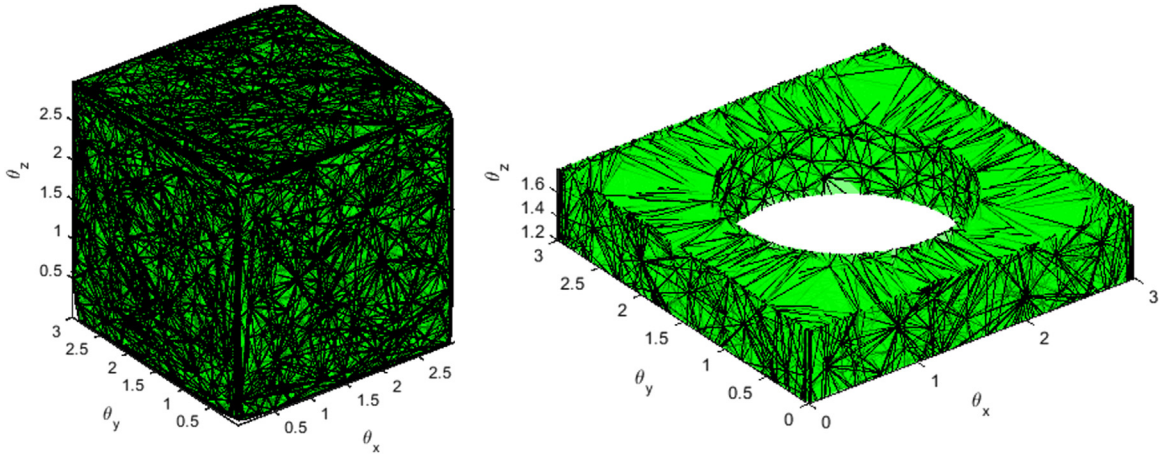

Fig. 15. Left – Triangulation scheme constructed according to 10^4 randomly generated proximity points; Right – Partial triangulation scheme shown for a limited range of θ_z.

$$FI_v = \frac{146.48}{(7.5+7.5)\times(15+15)} = 0.3255 \tag{17}$$

$$FI_v = \frac{146.46}{(7.5+7.5)\times(15+15)} = 0.3255 \tag{18}$$

By using the proposed search algorithm, the feasible region was characterized with 1000 feasible proximity points (see Fig. 11) and the corresponding triangulation scheme is given in Fig. 12. The area of feasible region was found to be 146.46 (which is 99.99% of the exact value). Thus the value of FI_v is

From the above results, it can be observed that the proposed algorithms can be easily implemented to produce accurate area estimates of non-simply connected regions at least in two-dimensional problems. On the other hand, although the simplicial approximation approach proposed by Goyal and Ierapetritou (2003) is also capable of handling

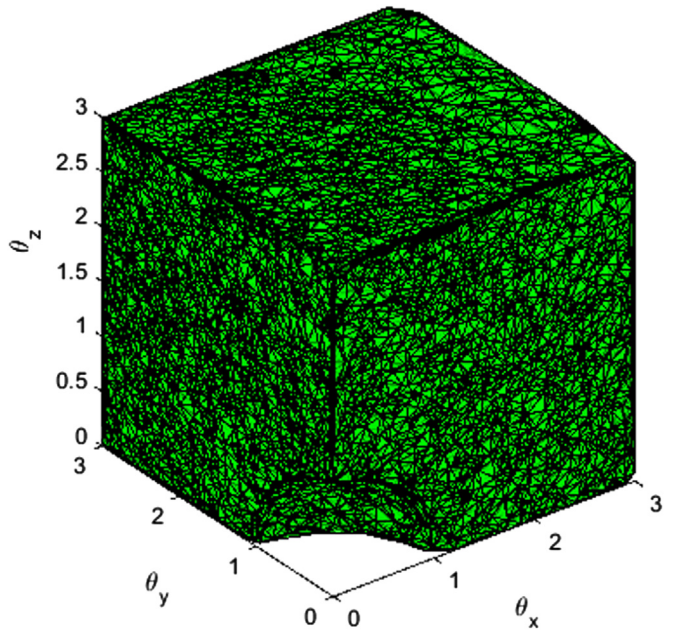

Fig. 16. Triangulation scheme constructed according to 10^4 randomly generated proximity points.

such regions, it is still necessary to identify the special geometric features of f_3, f_5, and f_6 in advance and, also, to construct the simplicial convex hull and outer convex polytope (Goyal and Ierapetritou, 2003).

For comparison purpose, the α-shape surface reconstruction computation Banerjee and Ierapetritou (2005) has also been repeated on the basis of 3217 evenly distributed points. The feasible area in this case is underestimated to be 141.23 units (which is 96.42% of the theoretical value) and, thus, the corresponding FI_v is 0.31. Although the α-shape surface reconstruction method was designed to handle the nonconvex and non-simply connected region, the estimation of its hypervolume is attainable only if a suitable α-shape factor can be identified properly. Furthermore, with more sampling points used (3217 points vs 1000 points), the estimation accuracy is actually lower than that achieved with the proposed method (96.42% vs 99.99% of the exact value).

4.3. 3D non-simply connected nonconvex feasible region

To show the effects of increasing proximity points, let us next consider a three-parameter feasible region bounded between a cube, i.e.,

$$\begin{aligned} f_1 &= \theta_x - 3 \le 0 \\ f_2 &= \theta_y - 3 \le 0 \\ f_3 &= \theta_z - 3 \le 0 \\ f_4 &= -\theta_x \le 0 \\ f_5 &= -\theta_y \le 0 \\ f_6 &= -\theta_z \le 0 \end{aligned} \tag{19}$$

and a sphere, i.e.,

$$f_7 = 1 - (\theta_x - 1.5)^2 - (\theta_y - 1.5)^2 - (\theta_z - 1.5)^2 \le 0 \tag{20}$$

where, θ_x, θ_y and θ_z are the uncertain parameters considered in the present example. The nominal point was placed at $\theta_x^N = \theta_y^N = \theta_z^N = 1.5$ and the expected positive and negative deviations in these uncertain parameters were chosen to be:

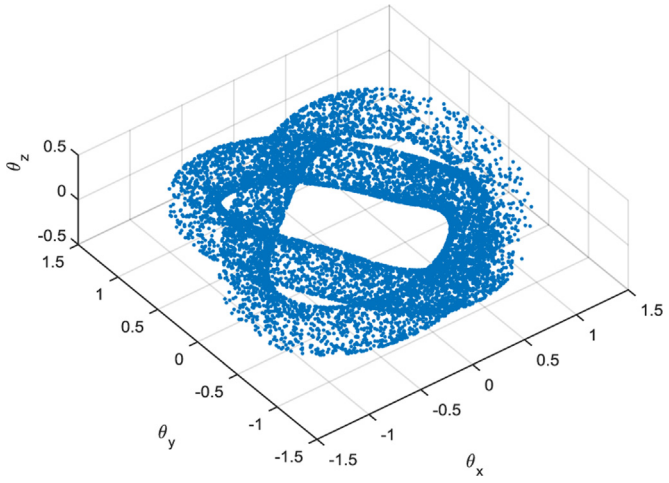

Fig. 17. 10^4 proximity points generated in 3D complicated feasible region.

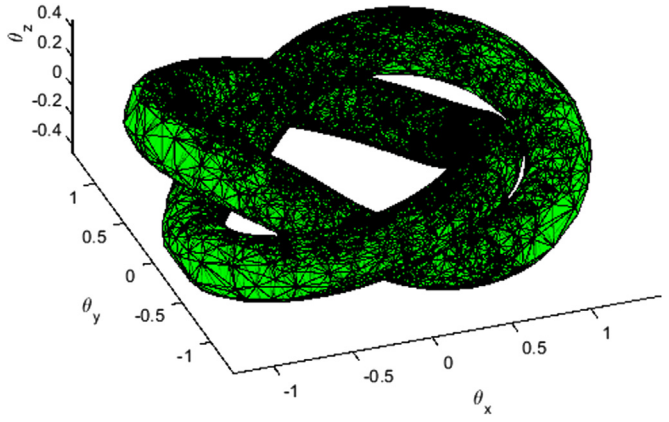

Fig. 18. Triangulation scheme constructed according to 10^4 randomly generated proximity points.

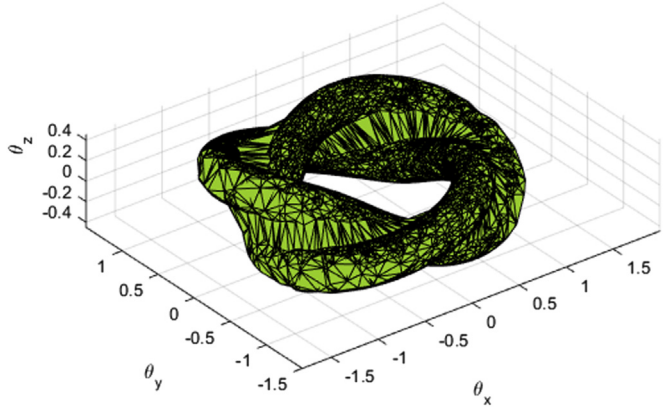

Fig. 19. Feasible region obtained with α-shape surface reconstruction.

$$\begin{aligned} \Delta\theta_x^+ &= \Delta\theta_x^+ = \Delta\theta_z^+ = 2.5 \\ \Delta\theta_x^- &= \Delta\theta_y^- = \Delta\theta_z^- = 1.5 \end{aligned} \tag{21}$$

The volume of this feasible region can be determined analytically to be 22.81 units, and thus the exact value of FI_v is 0.36.

Using the auxiliary vector approach (Lai and Hui, 2008), the spherical void inside the cube cannot be detected properly and, thus, an erroneous volume of 27 units was obtained. Note that the auxiliary vector approach calls for two objectives, i.e., (1) maximizing the sum of lengths of the position vectors that represent

Table 1
Computation results in higher-dimensional cases.

Case		Auxiliary vector (Lai and Hui, 2008)	Subspace feasibility test (Lai and Hui, 2008)	Proposed (10^n points[a])	CPU time needed to implement the proposed algorithm
Flow problem with five uncertain parameters	V_{fr}	23.81	29.22	29.30	14 min
	FI_v	0.744	0.913	0.92	
HEN problem with seven uncertain parameters	V_{fr}	118.4	126.72	126.22	4 h 36 min
	FI_v	0.925	0.99	0.99	

[a] n is chosen to be the dimension of the individual problem.

the interception points and (2) maximizing the sum of squares of the distances between interception points and a reference point. The maximum length of the position vectors is undoubtedly the corners of the cube, thus the sphere void is inevitably left undetected. If the other available methods, i.e., simplicial approximation and α-shape surface reconstruction, are applied in this case, the drawbacks described in the previous 2D example can also be observed. The former calls for a priori knowledge of the geometric features of the feasible region and also tedious steps to construct the simplicial convex hull and outer convex polytope, while the latter requires iterative tuning of the algorithm parameter but often yields lower accuracy.

By carrying out the proposed computation procedure, the feasible region can be described accurately. To show the resolution improvement achieved by introducing more proximity points, 10^2, 10^3 and 10^4 randomly generated points and their corresponding triangulation schemes are plotted in Fig. 13–15, respectively. The total volume of all simplexes in the most refined scheme in Fig. 15 has been calculated and used as the estimated volume of the feasible region. This estimate for 10^4 feasible proximity points is 22.83 units, which is 100.09% of the theoretical value, and the corresponding FI_v (0.36) is essentially the same as that determined analytically.

With fewer proximity points, i.e., 10^2 and 10^3 points, the volume of feasible region was estimated to be 18.53 units (81.24% of the theoretical value) and 22.92 (100.39% of the theoretical value), respectively. Note that, when compared with the results generated with the auxiliary vector approach (Lai and Hui, 2008), the boundaries of feasible region can be better characterized and the corresponding volume more accurately estimated by following the proposed computation procedure with 10^3 points (27 units vs 22.80 units). On the other hand, since it is obvious that 10^2 feasible proximity points cannot cover the entire feasible region adequately as shown in Fig. 13, the corresponding results are not satisfactory.

Finally, it can be observed from the results obtained in this 3-D problem and other extensive case studies that the feasible region can usually be better characterized with more proximity points until reaching a saturation level. A heuristic rule can thus be deduced to facilitate proper selection of the number of feasible proximity points, i.e., this number should at least be set at 10^n (where n is the dimension of parameter space) for rough estimations and may be raised to 10^{n+1} if a higher accuracy is desired. This suggested rule will also be tested in the subsequent examples.

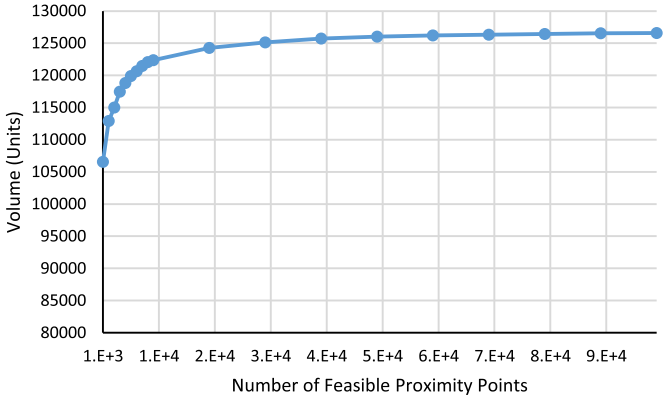

Fig. 20. Effects of increasing feasible proximity points in heat exchanger network example.

For direct comparison with previous works, let us next consider the following three-parameter system studied by Goyal and Ierapetritou (2003):

$$\begin{aligned} f_1 &= \theta_x - 3 \le 0 \\ f_2 &= \theta_y - 3 \le 0 \\ f_3 &= \theta_z - 3 \le 0 \\ f_4 &= 1 - \theta_x^2 - \theta_y^2 - \theta_z^2 \le 0 \\ f_5 &= -\theta_x \le 0 \\ f_6 &= -\theta_y \le 0 \\ f_7 &= -\theta_z \le 0 \end{aligned} \tag{22}$$

where the center of the sphere in prior example is located in the origin, i.e., (0, 0, 0). The nominal point was placed similarly at $\theta_x^N = \theta_y^N = \theta_z^N = 1.5$ and the expected positive and negative deviations in the uncertain parameters were chosen to be:

$$\begin{aligned} &\Delta\theta_x^+ = \Delta\theta_y^+ = \Delta\theta_z^+ = 2.5 \\ &\Delta\theta_x^- = \Delta\theta_y^- = \Delta\theta_z^- = 1.5 \end{aligned} \tag{23}$$

The volume of this region can be determined analytically to be 26.48 units, and thus the exact value of FI_v is 0.41.

The volume of feasible region was originally estimated to be 25.88 units (97.73% of the theoretical value) by Goyal and Ierapetritou (2003) and thus a conservative FI_v value of 0.40 was obtained. On the other hand, Lai and Hui (2008) studied the same problem and produced an even smaller volume estimate, i.e., 25.26 units (95.39% of the theoretical value), with the auxiliary vector approach and also a more conservative flexibility index (0.39).

Using the proposed method, the feasible region can be characterized with the 10^4 proximity points and the corresponding triangulation schemes are plotted in Fig. 16. The total volume of all simplexes has been calculated and used as the estimated volume of the feasible region. This estimate for 10^4 proximity points is 26.47 units, which is 99.96% of the theoretical value, and the corresponding FI_v (0.41) is essentially the same as that determined analytically. Note that, when compared with the results reported in Goyal and Ierapetritou (2003) and Lai and Hui (2008), the boundaries of feasible region can be better characterized and the corresponding volume more accurately estimated by following the proposed computation procedure.

4.4. 3D complicated feasible region

Let us consider a fictitious case when the feasible region is

defined in a very complicated way as follows (Klaus, 2010):

$$\begin{aligned}
&\Big(-8(\theta_x^2+\theta_y^2)^2(\theta_x^2+\theta_y^2+1+\theta_z^2+a^2-b^2)\\
&\quad+4a^2(2(\theta_x^2+\theta_y^2)^2-(\theta_x^3-3\theta_x\theta_y^2)(\theta_x^2+\theta_y^2+1))\\
&+8a^2(3\theta_x^2\theta_y-\theta_y^3)z+4a^2(\theta_x^3-3\theta_x\theta_y^2)\theta_z^2\Big)^2\\
&-(\theta_x^2+\theta_y^2)(2(\theta_x^2+\theta_y^2)(\theta_x^2+\theta_y^2+1+\theta_z^2+a^2-b^2)^2\\
&\quad+8(\theta_x^2+\theta_y^2)^2\\
&+4a^2(2(\theta_x^3-3\theta_x\theta_y^2)-(\theta_x^2+\theta_y^2)(\theta_x^2+\theta_y^2+1))\Big)\\
&-8a^2(3\theta_x^2\theta_y-\theta_y^3)\theta_z-4(\theta_x^2+\theta_y^2)a^2\theta_z^2\Big)^2=0\\
&0\le b\le 0.2\\
&-1.5\le\theta_x\le 1.5\\
&-1.5\le\theta_y\le 1.5\\
&-0.5\le\theta_z\le 0.5
\end{aligned}\tag{24}$$

The feasible region is actually a complicated object called *trefoil*. It will be very difficult to construct the simplicial convex hull and outer convex polytope (Goyal and Ierapetritou, 2003) based on Eq. (24). It will also be erroneous by auxiliary vector approach (Lai and Hui, 2008) since the method is limited by the number of search vectors available.

Using the proposed method, the feasible region can be characterized with the 10^4 feasible proximity points and the corresponding triangulation schemes are plotted in Figs. 17 and 18, respectively. The volume of feasible region was found to be 1.54 and the value of FI_v is

$$FI_v=\frac{1.54}{(1.5+1.5)\times(1.5+1.5)\times(0.5+0.5)}=0.1711 \tag{25}$$

Finally, the α-shape surface reconstruction operation (Banerjee and Ierapetritou, 2005) has also been repeated on the basis of the 10^4 proximity points generated by the proposed search algorithm. As shown in Fig. 19, this approach only yielded a poorly characterized feasible region.

4.5. A heat exchanger network with 4 uncertain parameters

To further demonstrate the effects of increasing feasible proximity points and the validity of the suggested heuristic rule, let us consider the heat exchanger network (HEN) design problem reported in Grossmann and Floudas (1987). The inequality constraints imposed in the original model are summarized below:

$$\begin{aligned}
f_1&=-0.67Q_c+T_3-350\le 0\\
f_2&=-T_5-0.75T_1+0.5Q_c-T_3+1388.5\le 0\\
f_3&=-T_5-1.5T_1+Q_c-2T_3+2044\le 0\\
f_4&=-T_5-1.5T_1+Q_c-2T_3-2T_8+2830\le 0\\
f_5&=T_5+1.5T_1-Q_c+2T_3+3T_8-3153\le 0
\end{aligned}\tag{26}$$

where T_1, T_3, T_5 and T_8 are uncertain parameters which denote the fluid temperatures at various locations in the network, and Q_c is a controllable load in the cooler. The nominal values of the above four temperatures are chosen at 620 K, 388 K, 583 K, and 313 K respectively in this example, while their expected positive and negative deviations are all set to be 10 K. Since there are four uncertain parameters in this example, the feasible region defined by Eq. (26) cannot be actually visualized with a 4-D plot.

Notice first that Lai and Hui (2008) have already studied this problem and produced the following results. Using the auxiliary vectors, they mapped every uncertain parameter to a standard interval of $[-1,+1]$ and found that the volume estimate of the normalized feasible region was 12.14 units and the corresponding FI_v was 0.76. It should be noted that the true volume can be calculated by multiplying the scale factors, i.e., $12.14\times10^4=121400$ units. Using the subspace feasibility tests, they divided the 4-D hypercube bounded by the expected upper and lower limits of uncertain parameters into 10,000 equal-sized hypercubic subspaces. The center of every subspace was then checked for feasibility. The flexibility index was calculated according to the following formula:

$$FI_v\approx\frac{N_{fs}}{N_s} \tag{27}$$

where, N_{fs} is the number of feasible subspaces and N_s is the total number of subspaces (which is 10,000 in this example). Note that this approach may require overwhelming computation resource and may lead to over/underestimation since the feasibility test is applied only to the center of each subspace. For the present example, FI_v was found to be 0.78.

The hypervolume of feasible region has also been estimated repeatedly according to the proposed computation procedure with different numbers of feasible proximity points. These estimates are plotted in Fig. 20 for 10^3–10^5 points. It can be observed that the estimated hypervolume starts to stabilize after increasing the point number to a value higher than 5×10^4. The hypervolume obtained with 5×10^4 and 10^5 points can be found to be 126623.13 and 126742.43 units, respectively, while the corresponding flexibility indices in both cases are almost the same, i.e., 0.79. Finally, note that the hypervolume at 10^4 points (122434.22 units) is in fact quite close to the converged value and, thus, the corresponding flexibility index (0.77) can be used as a rough estimate for preliminary analysis.

4.6. Feasible regions in higher dimensions

To show the superior capability of the proposed strategy in computing the hypervolumes of high-dimensional feasible regions, the following two examples are presented in the sequel:

i. a flow problem with five uncertain parameters (Grossmann and Floudas, 1987; Lai and Hui, 2008), and
ii. a HEN design problem with seven uncertain temperatures (Grossmann and Floudas, 1987; Lai and Hui, 2008).

For the sake of brevity, only the final results obtained with two available approaches, i.e., auxiliary vector and subspace feasibility test, and also the proposed procedure are presented in Table 1.

From these results one can see that: (1) the auxiliary vector approach usually underestimates the hypervolume of feasible region volume, (2) the subspace feasibility test is dependable but inefficient, since all subspaces in the entire parameter hypercube have to be checked exhaustively, and (3) the proposed method may be adopted to produce accurate estimates of V_{fr} and FI_v with reasonable computation effort. Since the CPU times needed by the available methods were not reported in literature, only the results obtained with the proposed algorithm are presented here. The long computational time in the second case was primarily due to the sequential steps performed in each MATLAB-GAMS calls (see Fig. 6), where in most cases each call only requires 0.001 s. If the steps in random line search, Delaunay Triangulation, infeasible check, and hypervolume calculation can be done in parallel, the total computation time can be reduced significantly. Furthermore, as the hardware price goes down continuously and parallel GPU computation becomes more

competitive, it is anticipated that the computational burden in higher dimensional problems can be alleviated gradually.

5. Conclusions

A new computation strategy is presented in this paper for evaluating the volumetric flexibility index of high-dimensional systems with enhanced accuracy. The random nature of line search results in precise characterization of the feasible region without a priori knowledge about its geometric properties. With Delaunay triangulation and infeasibility checks on the resulting simplexes, the hypervolumes of disjoint, non-simply connected and/or non-convex regions can be computed accurately and efficiently. A heuristic rule is also suggested to facilitate proper selection of the number of feasible proximity points. The effectiveness of the proposed computation strategy has also been clearly demonstrated in a series of case studies. Note finally that valuable practical information can be extracted from the feasible proximity points obtained from random line search. Each point can be associated with the neighboring condition of an active constraint or system's bottleneck. Potential revamp measures may then be adopted to relax the corresponding constraint so as to enhance flexibility.

References

Adi, V.S.K., Chang, C.T., 2011. Two–tier search strategy to identify nominal operating conditions for maximum flexibility. Ind. Eng. Chem. Res. 50, 10707–10716.

alphaShape [Internet]. Massachusetts: MathWorks, Inc.; c1994–2014 (cited 2014 Oct 10). Available from: ⟨http://www.mathworks.com/help/matlab/ref/alphashape.html⟩.

Banerjee, I., Ierapetritou, M.G., 2005. Feasibility evaluation of nonconvex systems using shape reconstruction techniques. Ind. Eng. Chem. Res. 44, 3638–3647.

Banerjee, I., Ierapetritou, M.G., 2002. Design optimization under parameter uncertainty for general black-box models. Ind. Eng. Chem. Res. 41, 6687–6697.

Banerjee, I., Ierapetritou, M.G., 2003. Parametric process synthesis for general nonlinear models. Comput. Chem. Eng. 27, 1499–1512.

Banerjee, I., Pal, S., Maiti, S., 2010. Computationally efficient black-box modeling for feasibility analysis. Comput. Chem. Eng. 34, 1515–1521.

Barber, C.B., Dobkin, D.P., Huhdanpaa, H.T., 1996. The Quickhull algorithm for convex hulls. ACM Trans. Math. Softw. 22, 469–483.

Bates, R.A., Wynn, H.P., Fraga, E.S., 2007. Feasible region approximation: a comparison of search cone and convex hull methods. Eng. Optimiz. 39, 513–527.

Boukouvala, F., Ierapetritou, M.G., 2012. Feasibility analysis of black-box processes using an adaptive sampling Kriging-based method. Comput. Chem. Eng. 36, 58–368.

Burkardt, J. Geometry: Geometric calculations (Internet). Florida: Department of Scientific Computing, Florida State University, (cited 2014 Oct 10). Available from ⟨http://people.sc.fsu.edu/~jburkardt/m_src/geometry/geometry.html⟩.

Chen, K., Anthony, S.M., Granick, S., 2014. Extending particle tracking capability with Delaunay triangulation. Langmuir 30, 4760–4766.

criticalAlpha (Internet), 2014. Massachusetts: MathWorks, Inc.; c1994–2014 (cited 2014 Oct 10). Available from: ⟨http://www.mathworks.com/help/matlab/ref/alphashape.criticalalpha.html⟩.

Croft, H.T., Falconer, K.J., Guy, R.K., 1991. Unsolved problems in geometry. In: Halmos, P.R. (Ed.), Problem Books in Mathematics. Springer Science+Business Media, New York.

Delaunay triangulation (Internet), 2014. Massachusetts: MathWorks, Inc.; c1994–2014 (cited 2014 Oct 10). Available from: ⟨http://www.mathworks.com/help/matlab/math/delaunay-triangulation.html⟩.

delaunayn (Internet), 2014. Massachusetts: MathWorks, Inc.; c1994–2014 [cited 2014 Oct 10]. Available from: ⟨⟨http://www.mathworks.com/help/matlab/ref/delaunayn.html⟩.

Dinas, S., Banon, J.M., 2014. A review on Delaunay triangulation with application on computer vision. Int. J. Comp. Sci. Eng. 3, 9–18.

Dirkse, S, Ferris, MC, Ramakrishnan, J., 2014. GDXMRW: Interfacing GAMS and MATLAB [Internet]. Washington DC: GAMS Development Corporation (updated 2014 Jul 11; cited 2014 Oct 10). Available from ⟨⟨http://www.gams.com/dd/docs/tools/gdxmrw.pdf⟩.

Goyal, V., Ierapetritou, M.G., 2003. Framework for evaluating the feasibility/operabiltiy of nonconvex processes. AIChE J. 49, 1233–1240.

Grossmann, I.E., Floudas, C.A., 1987. Active constraint strategy for flexibility analysis in chemical process. Comput. Chem. Eng. 11, 675–693.

Ierapetritou, M.G., 2001. A new approach for quantifying process feasibility: convex and one dimensional quasi-convex regions. AIChE J. 47, 1407–1417.

Ierapetritou, M.G., 2009. Bilevel optimization: Feasibility test and flexibility index. In: Floudas, C.A., Pardalos, P.M. (Eds.), Encyclopedia of Optimization. Springer, New York, pp. 228–239.

Johnson, R.A., 2007. Advanced euclidean geometry. Dover Publications, New York.

Klaus, S., 2010. The solid trefoil knot as an algebraic surface. CIM Bull. 28, 2–4.

Krantz, S.G., 1999. Handbook of Complex Variables. Birkhäuser, Boston.

Lai, S.M., Hui, C.-W., 2008. Process flexibility for multivariable systems. Ind. Eng. Chem. Res. 47, 4170–4183.

Lima, F.V., Jia, Z., Ierapetritou, M.G., Georgakis, C., 2010. Similarities and differences between the concepts of operability and flexibility: the steady-state case. AIChE J. 56, 702–716.

MATLAB, 2014. The Language of Technical Computing (Internet). Massachusetts: MathWorks, Inc.; c1994–2014 (cited 2014 Oct 10). Available from: ⟨http://www.mathworks.com/products/matlab/⟩.

Riyanto, E., Chang, C.T., 2010. A heuristic revamp strategy to improve operational flexibility of water networks based on active constraints. Chem. Eng. Sci. 65, 2758–2770.

Rogers, A., Ierapetritou, M., 2015a. Feasibility and flexibility analysis of black-box processes Part 1: surrogate-based feasibility analysis. Chem. Eng. Sci. 137, 986–1004.

Rogers, A., Ierapetritou, M., 2015b. Feasibility and flexibility analysis of black-box processes Part 2: surrogate-based flexibility analysis. Chem. Eng. Sci. 137, 1005–1013.

Rosenthal, R.E., 2014. GAMS — A user's guide. Tutorial by Richard E. Rosenthal [Internet]. Washington DC: GAMS Development Corporation; c2014 (updated 2014 Sept; cited 2014 Oct 10). Available from ⟨http://www.gams.com/dd/docs/bigdocs/GAMSUsersGuide.pdf⟩.

Stein, P., 1966. A note on the volume of a simplex. Am. Math. Mon. 73, 299–301.

Swaney, R.E., Grossmann, I.E., 1985a. An index for operational flexibility in chemical process design. Part I: formulation and theory. AIChE J. 31, 621–630.

Swaney, R.E., Grossmann, I.E., 1985b. An index for operational flexibility in chemical process design. Part II: computational algorithms. AIChE J. 31, 631–641.

Vempala, S., 2005. Geometric random walks: a survey. In: Goodman, J.E., Pach, J., Welzl, E. (Eds.), Combinatorial and Computational Geometry 52. Cambridge University Press, New York, pp. 573–612.

Yazdchi, K., Bertoldi, K., Luding, S., 2009. Application of Delaunay triangulation in numerical simulation of discrete particle systems. EM Symposium, Lunteren.

Zhou, W., Yan, H., 2012. Alpha shape and Delaunay triangulation in studies of protein-related interactions. Brief Bioinform. 15, 54–64.

Zilinskas, A., Fraga, E.S., Mackute, A., 2006. Data analysis and visualisation for robust multi-criteria process optimisation. Comput. Chem. Eng. 30, 1061–1071.